Submitted: 18/01/2024
Accepted: 03/13/2024
Published: 04/05/2024

Research Article

[1]School of Physics, University of Bristol, Bristol, United Kingdom

Keywords

Accretion discs, black holes, thick discs, accretion flows

Email Correspondence

zo20222@bristol.ac.uk

https://doi.org/10.26443/msurj.v19i1.229

Wiktoria Tarnopolska[1]

Properties of Accretion Discs Around Black Holes through Modelling

Abstract

We examine accretion discs within the context of Einstein's general relativity. We use the metrics corresponding to the four black hole solutions proposed by Einstein, with the Shakura-Sunyaev model of the disc. Starting from the definition of the "no-hair theorem" that a black hole only stores information about three main parameters — mass, angular momentum and charge – we tested the impact of varying these parameters, emphasising the relations between them. Moreover, the research we present here captures and illustrates two pivotal aspects predicted by general relativity: the circular photon ring and the frame-dragging effects of the ergosphere. Our research delves into emissivity profiles, exploring both the well-established lamp post model and the beamed point source model. We reproduced the results from the literature and noted the inconsistencies between the works and our results while also providing an alternative source supporting our results. Altogether, this work presents a comprehensive exploration of accretion disc dynamics around central compact objects within the framework of Einstein's general relativity, shedding light on intricate phenomena that continue to captivate the scientific community.

Introduction

Black holes, with their unparalleled gravitational force, stand as some of the most enigmatic objects in the Universe. Their intense gravitational pull has made it challenging to scrutinize them through direct observation. It was not until 2019 that the groundbreaking work of the Event Horizon Telescope provided the first visual confirmation of a black hole's existence in the Messier 87 galaxy[1]. Nevertheless, the theoretical groundwork for black holes had been laid long before, rooted in mathematical and theoretical models that predicted their existence.

The currently prevailing belief, resulting from work in the late 20th century, is that dense star clusters and massive stars have an almost inexorable destiny of collapsing into black holes. This hypothesis suggests the likely existence of supermassive black holes at the cores of galaxies, especially if they have been active[2]. Beyond their role in cosmic architecture, black holes serve as astonishingly efficient power sources. Accretion onto a black hole stands as the most efficient process known for emitting energy. Of particular note are Kerr rotating black holes, renowned for their exceptional power. Accretion onto a Kerr black hole is actually the most efficient process in the Universe, with efficiency 0.426 for a maximally rotating black hole in the Kerr metric[3].

Methods

`Gradus.jl`[4] is a novel photon ray tracing code authored by Baker & Young (2022) and proves to be an essential tool in black hole modelling. This software enables a range of numerical simulations, with a primary focus on exploring various accretion disc scenarios. We used a new photon integration code to investigate photon orbits around the black holes, since the `Gradus` code allows arbitrary spacetime metrics to be used in a straightforward manner. We focused on the four distinct black holes solutions arising from general relativity, with particular emphasis on Kerr, Kerr-Newman, and Reissner-Nordstrom metrics. These simulations provided a platform for testing the "no-hair theorem" by testing the effects of varying the three black hole parameters – mass M, angular momentum J and charge Q –predicted by the theorem to be the only information characterising a black hole. We used point-source ray tracing, and reconfigured the present lamp post model to represent a flare within the accretion disc. This enabled investigation of how photon trajectories are influenced by the presence of singularities in different metrics.

Furthermore, by using and modifying `Gradus.jl`, we simulated emissivity profiles both for a stationary and a beamed point source, as well as line profiles for black holes of varying spin and charge parameters.

Testing the No-Hair Theorem

In 1972, Jacob Bekenstein first introduced the "no-hair theorem," a concept later revised in 1995. This theory postulates that black holes possess minimal characteristics, encompassing only three fundamental components: mass M, angular momentum J, and charge Q. Remarkably, John A. Wheeler, who famously coined the term "black hole," drew upon Bekenstein's "no-hair" concept to propose an intriguing notion. Wheeler suggested that if two black holes shared identical values of momentum, charge, and mass, yet one was composed of matter while the other consisted of antimatter, they would be indistinguishable, as outlined in his work[5].

The intriguing consequence of the no-hair theorem's violation is the disruption of symmetry, leading to the transformation of the photon ring's shape. Johannsen & Psaltis[6] state that the degree of asymmetry is a direct measure of the violation of the "no-hair theorem." Furthermore, research conducted

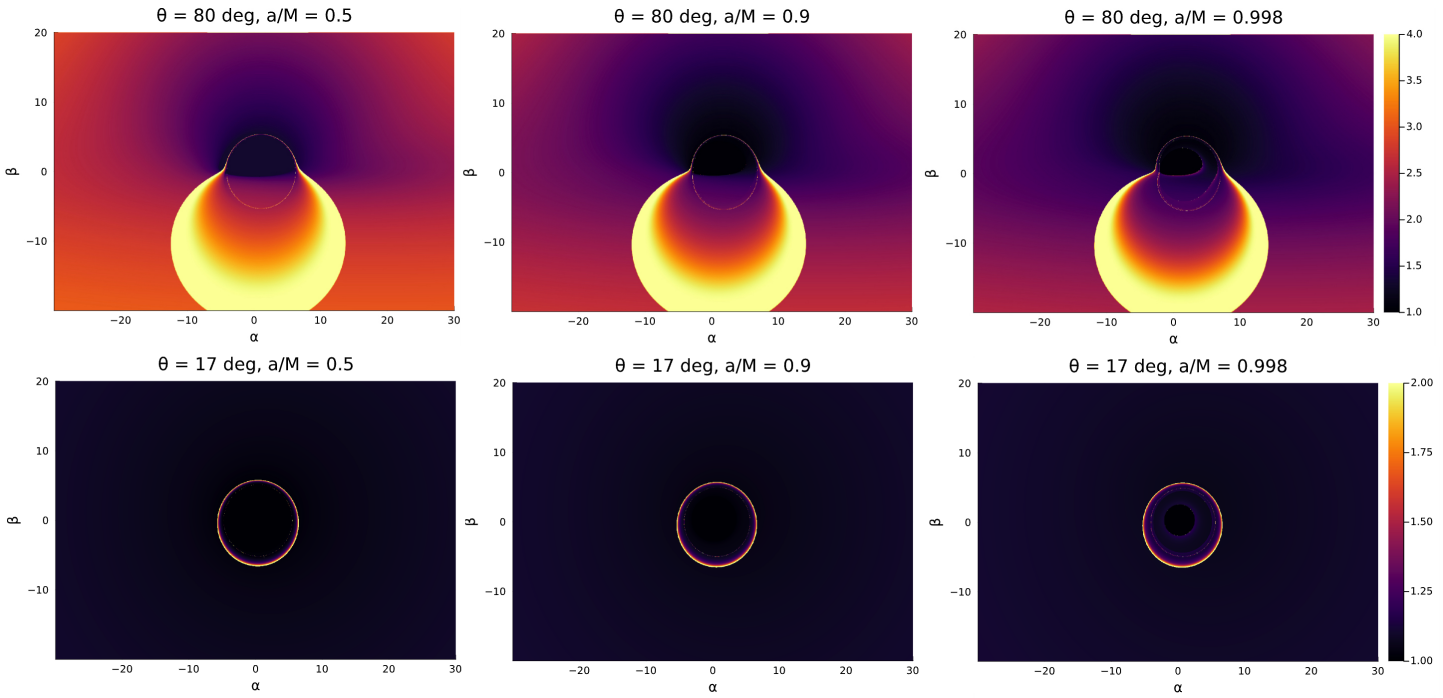

Figure 1. Effects of varying the a/M ratio for a rotating Kerr black hole, increased from left to right, with α and β representing the impact parameters. The first row shows the black hole as viewed from an inclination angle of 80° and the row below with the observer at an inclination angle of 17°. The shape of the photon ring becomes increasingly asymmetric and offset from the origin, remaining almost circular for $a \leq 0.9M$ and losing the circular shape for a rapidly rotating black hole at $a/M = 0.998$.

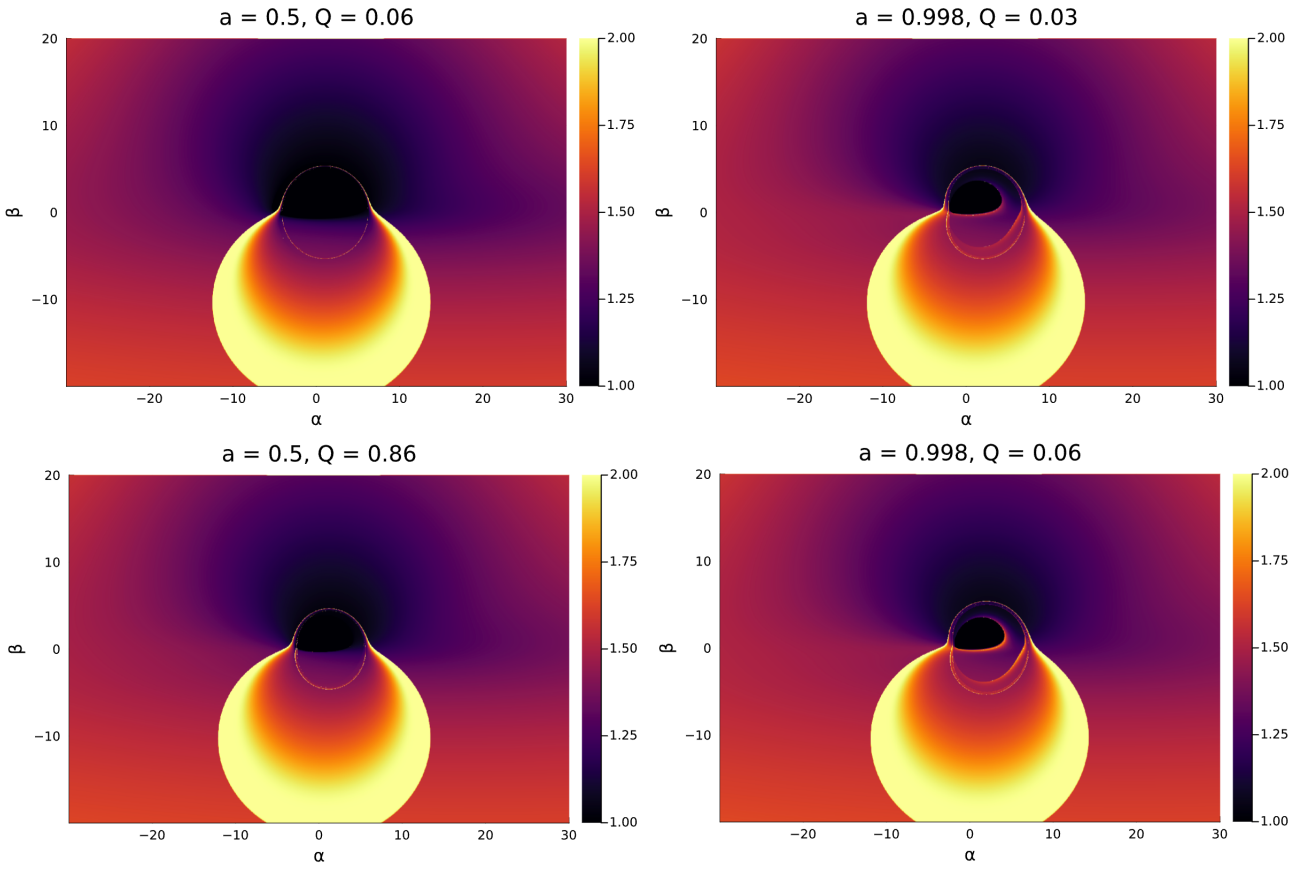

Figure 2. Results of varying charge for black holes in the Kerr–Newman metric with spin $a/M = 0.5$ (left) and $a/M = 0.998$ (right). Deformation of the photon ring is observed as the charge is increased for the $a = 0.5$ case while for the rapidly rotating $a = 0.998$ black hole, increased radiative transfer is observed "inside" the photon ring.

by Bambi & Freese[7] explored the possibility of using the black hole images to test if black holes with $a \leq M$ violate the "no-hair theorem," depending on whether general relativity remains valid in this strong field regime. Specifically, in the case of a Schwarzschild non-rotating black hole, the photon ring becomes elliptical. For a rotating Kerr black hole, this asymmetry becomes even more pronounced, as detailed by the research conducted by Johannsen & Psaltis[6]. Using the computational capabilities of `Gradus.jl`, we validated these findings. Our investigation demonstrates that, within the Kerr metric framework, the ring remains virtually circular for values of spin $a \leq 0.9M$, where $a = J/M$ with increased asymmetry observed at higher values.

While the Kerr metric serves as the spinning extension of the Schwarzschild solution, the Kerr-Newman spinning-charged solution represents both a charged generalization of the Kerr metric and a spinning counterpart to the Reissner-Nordstrom solution. Collectively, these four metrics constitute the cornerstone of the black hole solutions of general relativity[8].

Results

Kerr metric

The Kerr metric serves as a spinning generalization of the Schwarzschild solution[9]. Within the framework of the Kerr metric, Figure 1 illustrates the effects stemming from variations in the spin-to-mass ratio (a/M) from the vantage points of two distinct observers. In Figures 1, 2, 3, the colours correspond to energy flux and the parameters α and β span the grid of the impact parameters and each pixel on the grid is coloured in the units proportional to units of intensity. As pointed out by Johannsen & Psaltis, as the a/M ratio is increased, the photon ring's symmetry diminishes. Upon reaching the maximum spin value of $a = 0.998$, the once-circular photon ring undergoes a significant transformation, becoming highly asymmetric and displaced from its original position. This transformation is a consequence of the black hole's ability to warp spacetime and induce frame-dragging, a phenomenon that occurs within the ergosphere of a black hole. This characteristic feature is described by the Kerr and Kerr–Newman metrics, which pertain to rotating black holes[10].

Kerr–Newman metric

The Kerr-Newman metric introduces a charge parameter Q into the description of a rotating black hole with non-zero spin. This mathematical framework captures the intricate interaction between gravitational and electromagnetic fields emanating from a rotating mass with an electric charge distributed along its axis of symmetry. Notably, the Kerr-Newman metric characterizes a rotating mass endowed with an electric charge, an extension originally crafted by Newman et al. in 1965[11], thereby arguing for the existence of the broader Kerr family of solutions.

It is worth noting that in astrophysical contexts, the electric charge of black holes is typically considered negligible. However, despite its minor role in natural astrophysical scenarios, accounting for electric charge remains valuable in theoretical modelling. Charge possessed by a black hole can still impact charged particles in the disc.

Plots were generated to illustrate four scenarios involving a charged rotating black hole within the Kerr–Newman metric framework. Two where $a/M = 0.5$, with values of Q set to 0.06 and 0.86 and two of a rapidly rotating black hole with $a/M = 0.998$ and charge 0.03 and 0.06 as depicted in Figure 2. Analogous to the scenario in the Kerr metric, these plots reveal frame dragging within the ergosphere and a distortion in the circular shape of the photon ring.

It is important to note the constraint

$$a^2 + Q^2 \leq M^2 \tag{1}$$

where equality holds for the extremal black hole[12], which originates from the Kerr solution itself. This condition ensures that the black hole's properties remain consistent with the underlying spacetime geometry. Taking this constraint into account, for a black hole with a spin parameter of $a = 0.5$, the maximum permissible charge is approximately $Q = 0.86$, while for a rapidly rotating black hole with $a = 0.998$, the maximum charge decreases significantly to around $Q = 0.06$.

Reissner–Nordström metric

Reissner-Nordström introduces the charge parameter Q as a specific instance of the Kerr-Newman metric. According to Misner[13], all static (i.e. non-rotating) black holes are distinctly defined by the parameters M and Q, and they exhibit the Reissner–Nordström form. The charged generalization of the Schwarzschild solution was independently uncovered by Reissner (1916) and Nordström (1918)[11]. There are no other existing solutions for stationary black holes.

The formula for the black hole shadow size as a function of its charge was derived in Zakharov[14] as

$$D = -512 \cdot \left(Q - \frac{9}{8}\right)^3 \tag{2}$$

where D is the shadow diameter and Q is the charge in units of mass M.

We created a black hole in Reissner–Nordström metric (Figure 3) and varied the charge to examine how the appearance of a black hole depends on Q. As predicted from the formula in the Equation 2, as the charge is increased, the diameter of the shadow decreases.

Point Source Ray Tracing

`Gradus` can simulate various corona models, including the lamp post model. By adapting the code to this model, we scrutinized the behavior of photons and their trajectories as if they emanated from an isotropic point source, and traced their paths to the accretion disc. Ray tracing is emerging as a powerful tool. Specifically, it facilitates the generation of images at remarkably high resolutions, allowing for a detailed examination of the substructure within the photon ring, as well as the influence of turbulence. The distinctive properties of photon subrings can be investigated[15] by employing an adaptive scheme and subring decomposition.

The results obtained from tracing these photon paths provide valuable insights into how altering the spin parameter (a) changes the behavior of black holes and the nearby photon paths. Notably, as the spin increases, the event horizon's diameter decreases in the Kerr metric. Despite the fact that the faster rotation of the black hole induces greater spacetime curvature due to frame-dragging (as illustrated in Figure 4), we observed photon paths to be less bent by a black hole with a smaller diameter, while the distance of the flare from the singularity remained constant. This phenomenon is attributed to the decreasing innermost stable circular orbit (ISCO) with increasing spin, which causes the photon orbit's radius to be smaller than that of a Schwarzschild black hole. In the latter case, the ISCO can be found at approximately three times the Schwarzschild radius ($3r_S$) before spiraling beyond the event horizon.

Emissivity Profiles

The corona is situated above the black hole and continuously emits X-rays that subsequently illuminate the accretion disc. This process generates a

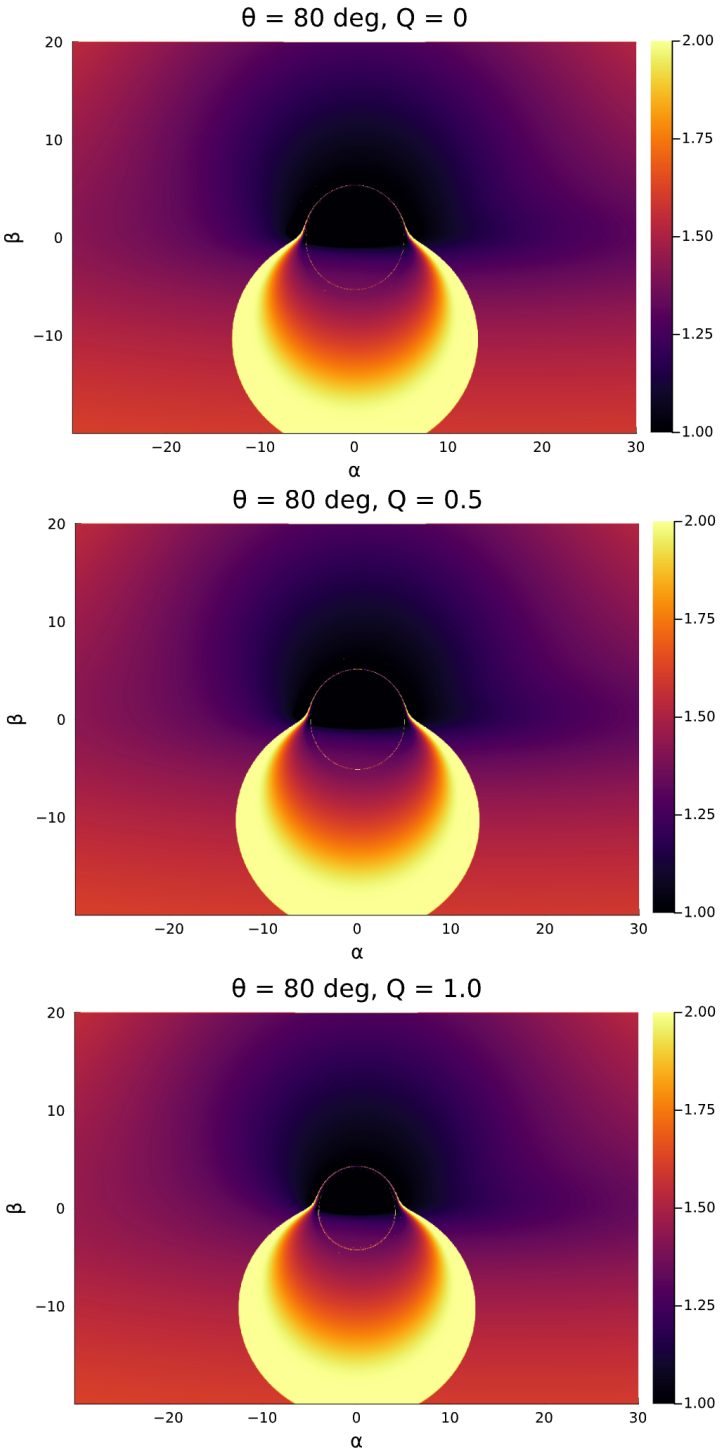

Figure 3. Energy flux of the Reissner–Nordström black hole with charge varied between 0 and 1. The first image at the top is the case of vanishing charge which, combined with absence of spin, illustrates the Shwarzschild metric for comparison. The results imply that the black hole shadow diameter decreases when charge Q is increased, which is consistent with literature.

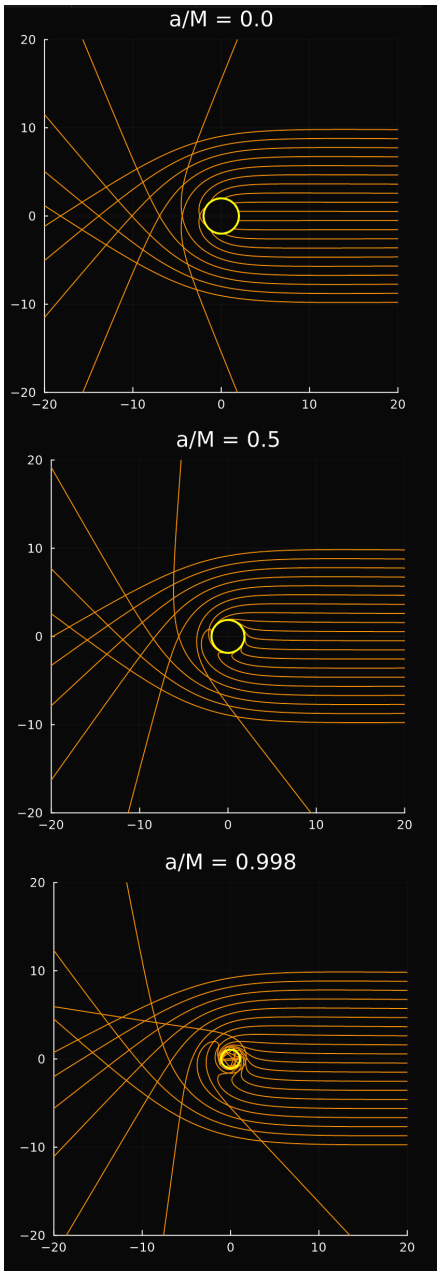

Figure 4. Frame dragging can be observed around rotating black holes, making a significant difference compared to a Schwarzschild black hole with $a/M = 0$.

discernible pattern interpreted as the emissivity profile. This profile depends on various factors, including the precise location and geometry of the X-ray source, as well as the characteristics of the accretion disc[16].

Using the `Gradus` tool, we replicated models proposed by Gonzalez et al. in 2017[17]. Our objective was to discern how the emissivity profile relies on parameters such as the height above the black hole, the displacement axis, and the photon index within the lamp post model. Furthermore, we examined insights from Dauser et al. 2013[18] on beamed point sources.

Results

Stationary lamp post

We simulated a Kerr black hole with a spin parameter of $a = 0.998$, representing the maximally rotating case. We employed the lamp post model to emulate the corona.

We systematically varied the height h of the radiation source within the range of 2.5 to 20 Schwarzschild radii, as illustrated in Figure 5. In the case of low resolution, which manifests as irregularities in the line plots, increasing the number of samples should resolve the issue, albeit at the cost of greater computation time. The results are consistent with existing literature findings[17,19]. Notably, the steepest slope in the observed emissivity profile

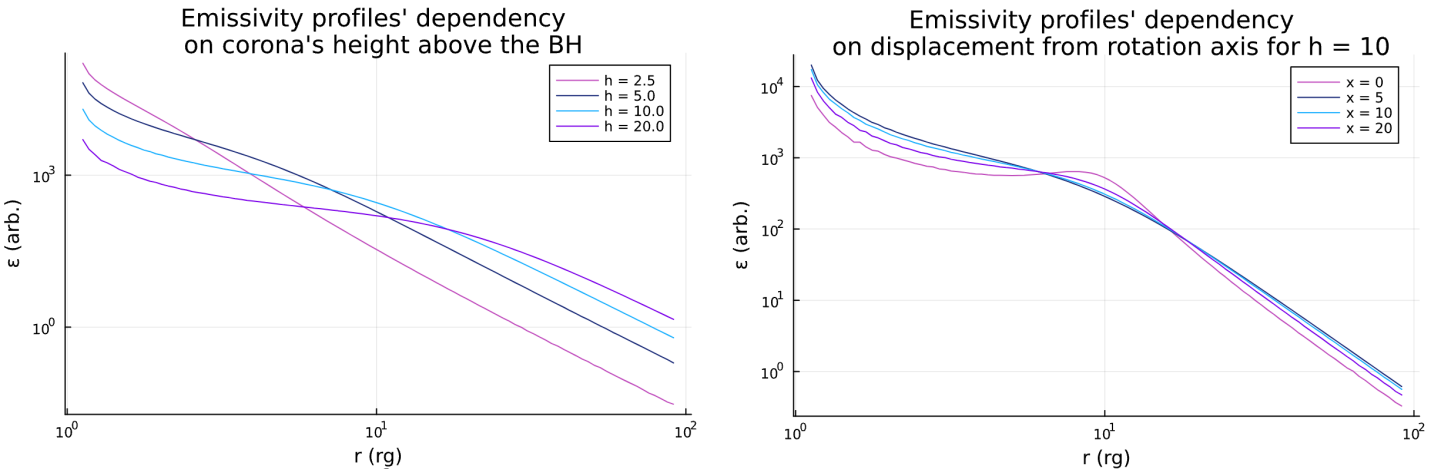

Figure 5. Results of varying corona's height (left) and displacement from rotation axis (right) above the black hole and accretion disc. First plot becomes more steep as the height is increased and the second shows that largest number of photons land under the source since as the corona is displaced from the rotation axis, outer disc receives more photons than the innermost parts and therefore becomes more illuminated.

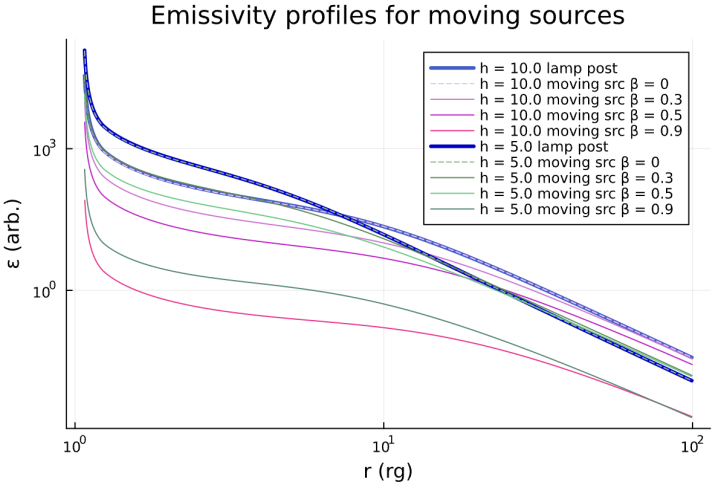

Figure 6. Emissivity profiles for sources at heights $h = 5$ and $h = 10$ with varying velocity of the jet base β. Includes 'tests' by comparing a stationary lamp post (blue) with a beamed source models with $\beta = 0$ (dashed) to show that the beamed point source model satisfies the predictions and to prove its correctness and consistency within the software as a whole.

corresponds to the source positioned closest to the black hole ($h = 2.5$ Schwarzschild radii). As the source distance increases, a diminishing slope is observed due to time dilation effects that enhance the flux of photons reaching the innermost region of the accretion disc[17].

Furthermore, the displacement of the radiation source from the rotation axis also influences the emissivity profile, as depicted in Figure 5. Axisymmetric system implies a disk-like of ring-shaped corona. Novel models provided within `Gradus.jl` calculate emissivity profiles in two-dimensional space on the disc, allowing us to analyse non-axisymmetric systems. Using the Voronoi decomposition of the disc, the profile is calculated and in the limit of large sample points approaches the true emissivity function. This displacement accentuates the discontinuity in the plot as it increases. The reason behind this behavior is that as the source moves away from the innermost section of the accretion disc, the outer regions become increasingly illuminated, with more photons impinging upon the disc beneath the source[17].

Beamed point source

Aside from stationary sources as found in the stationary lamp model, beamed sources play a crucial role, particularly in active galactic nuclei (AGN) exhibiting jet-like structures or outflows. Given that point sources are among the most likely candidates to exhibit beaming effects, we formulated a model of a beamed point source. The corona begins at a designated height h and can subsequently be projected upward with a velocity β (note: not the impact parameter as before). To simulate this model, we modified the `Gradus` code. We introduced a new datatype that enables the specification of a corona that dynamically moves away from the vicinity of the black hole. This feature has now been successfully implemented within the software.

However, the results obtained from the beamed source (Figure 6) do not align with those reported in literature[17,19]. Furthermore, when examining the moving source plots in Fig. 6(c) in Gonzalez et al. (2017)[17], and Fig. 11 in Wilkins et al. (2012)[19], the two datasets do not agree either, despite the sole variation being the height of the corona.

Gonzalez et al. report that a sudden drop is observed in emissivity over the middle region of the disc due to relativistic effects caused by the beamed source[17]. The same was not reported by Wilkins et al.[19]. Wilkins et al. do not describe in detail their method for calculating these beamed point source emissivities[19]. On the other hand, the tetrad calculation by Gonzalez et al. is consistent with the one implemented in `Gradus.jl`, and the local momenta are consistent with Wilkins et al. However, the outcomes presented in Figure 6 ultimately agree with those reported in Fig. 6(a) of Dauser et al. (2013)[18]. The trends we observed are consistent and the quantitative comparison will be performed in the future. As the height of the jet base increases, the plot shifts downward, and with an increase in velocity, it becomes less steep. This suggests that the photon flux diminishes with higher speeds, as photons are propelled away from the accretion disc.

Conclusion

In conclusion, employing powerful computational tools such as `Gradus.jl`, yielded profound insights into the behaviour of black holes and their interaction with the spacetime and photons. Through intricate simulations based on established metrics such as Kerr, Kerr-Newman, and Reissner-Nordström, the study has not only validated key theoretical predictions but also expanded the understanding of these objects and the

results coming from the environment they create.

The definition of the "no-hair theorem" states that a black hole only stores information about three parameters — mass, angular momentum and charge. The impact of varying these parameters on the photon ring's shape, as demonstrated through simulations, emphasises the relations between the three black hole parameters.

The application of point-source ray tracing allowed us to observe and justify the intricate behaviour of photons in close proximity of black holes. Moreover, the study of emissivity profiles, both from stationary and beamed point sources, has provided valuable insights into the intricate dynamics of accretion flows.

Navigating through the implications of black holes parameters such as height, displacement, and velocity in the simulations, the significance of the versatility of tools like `Gradus.jl` becomes apparent. Computational simulations notably serve as a bridge connecting theoretical predictions with observable phenomena, offering a unique way of analysing black holes in diverse astrophysical contexts.

Acknowledgements

In this article, I would like to specifically honour the memory of my beloved Grandfather, Zbigniew Komorowski, who passed away in October of 2022. He was a great man without whom I would not be where I am today and I will always be grateful for his support, love and sharing his passion for science. I am honoured to be able to celebrate his memory in this beautiful way.

Special thanks to Professor Andrew Young for his help and guidance, feedback and supervision of this project. Extending my sincere thanks to Fergus Baker, the mind behind Gradus, for countless code checks, support and collaboration during my work.

I would like to express my deep gratitude for a grant from the Royal Astronomical Society that financed my research this summer alongside funding from the University of Bristol.

References

1. Akiyama, K. et al. First M87 event horizon telescope results. IV. Imaging the central supermassive black hole. *Astrophys. J. Lett.* **875,** L4 (2019). https://doi.org/10.3847/2041-8213/ab0e85
2. Rees, M. J. Black hole models for active galactic nuclei. *Annu. Rev. Astron. Astrophys.* **22,** 471–506 (1984). https://doi.org/10.1146/annurev.aa.22.090184.002351
3. Choudhury, M. Black Holes and the Scientific Process. Preprint at https://doi.org/10.48550/arXiv.1506.01957 (2015).
4. Baker, F. & Young, A. *Gradus.jl* version 0.1.0. 2022. https://doi.org/10.5281/zenodo.6471796.
5. Ruffini, R. & Wheeler, J. A. Introducing the black hole. *Phys. Today* **24,** 30–41 (1971). http://dx.doi.org/10.1063/1.3022513
6. Johannsen, T. & Psaltis, D. Testing the no-hair theorem with observations in the electromagnetic spectrum. II. Black hole images. *Astrophys. J.* **718,** 446–454 (2010). https://doi.org/10.1088/0004-637X/718/1/446
7. Bambi, C. & Freese, K. Apparent shape of super-spinning black holes. *Phys. Rev.* **79,** 043002 (2009). https://doi.org/10.1103/PhysRevD.79.043002
8. Adamo, T. & Newman, E. T. The Kerr-Newman metric: A Review. *Scholarpedia* **9,** 31791 (2014). htttps://doi.org/10.4249/scholarpedia.31791
9. Kerr, R. P. Gravitational field of a spinning mass as an example of algebraically special metrics. *Phys. Rev. Lett.* **11,** 237–238 (1963). htttps://doi.org/10.1103/PhysRevLett.11.237
10. Wex, N. & Kopeikin, S. M. Frame dragging and other precessional effects in black hole pulsar binaries. *Astrophys. J.* **514,** 388 (1999). http://dx.doi.org/10.1086/306933
11. Wald, R. M. *General Relativity* chap. 8 (University of Chicago Press, 1984).
12. Liu, C. Q. Collision of two general geodesic particles around a Kerr–Newman black hole. *Chin. J. Phys.* **30,** 100401 (2013). https://doi.org/10.1088/0256-307X/30/10/100401
13. Misner, C. W., Thorne, K. S. & Wheeler, J. A. *Gravitation* chap. 33 (W. H. Freeman and Company, 1973).
14. Zakharov, A. F. Constraints on a charge in the Reissner-Nordström metric for the black hole at the Galactic Center. *Phys. Rev.* **90,** 062007 (2014). https://doi.org/10.1103/PhysRevD.90.062007
15. Gelles, Z. et al. The Role of Adaptive Ray Tracing in Analyzing Black Hole Structure. *Astrophys. J.* **912,** 39 (2021). http://dx.doi.org/10.3847/1538-4357/abee131
16. Wilkins, D. R. & Fabian, A. C. Determination of the X-ray reflection emissivity profile of 1H 0707-495. *Mon. Not. R. Astron. Soc.* **414,** 1269–1277 (2011). http://dx.doi.org/10.1111/j.1365-2966.2011.18458.x
17. Gonzalez, A. G. et al. Probing the geometry and motion of AGN coronae through accretion disc emissivity profiles. *Mon. Not. R. Astron. Soc.* **472,** 1932–1945 (2017). http://dx.doi.org/10.1093/mnras/stx2080
18. Dauser, T. et al. Irradiation of an Accretion Disc by a Jet: General Properties and Implications for Spin Measurements of Black Holes. *Mon. Not. R. Astron. Soc.* **430,** 1694–1708 (2013). http://dx.doi.org/10.1093/mnras/sts710
19. Wilkins, D. R. & Fabian, A. C. Understanding X-ray reflection emissivity profiles in AGN: locating the X-ray source. *Mon. Not. R. Astron. Soc.* **424,** 1284–1296 (2012). http://dx.doi.org/10.1111/j.1365-2966.2012.21308.x